A three-dimensional time-dependent theory for helix traveling wave tubes in beam-wave interaction*

Peng Wei-Feng(彭维峰), Hu Yu-Lu(胡玉禄), Yang Zhong-Hai(杨中海), Li Jian-Qing(李建清), Lu Qi-Ru(陆麒如), and Li Bin(李 斌)†

Vacuum Electronics National Laboratory, University of Electronic Science and Technology of China, Chengdu 610054, *China*

(Received 21 April 2010; revised manuscript received 15 July 2010)

This paper presents a three-dimensional time-dependent nonlinear theory of helix traveling wave tubes for beam-wave interaction. The radio frequency electromagnetic fields are represented as the superposition of azimuthally symmetric waves in a vacuum sheath helix. Coupling impedance is introduced to the electromagnetic field equations' stimulating sources, which makes the theory easier and more flexible to realize. The space charge fields are calculated by electron beam space-charge waves expressed as the superposition solutions of Helmholtz equations. The focusing forces due to either a solenoidal field or a periodic permanent magnetic field is also included. The dynamical equations of electrons are Lorentz equations associating with electromagnetic fields, focusing fields and space-charge fields. The numerically simulated results of a tube are presented.

Keywords: helix traveling wave tubes, time-dependent theory, sheath helix, space-charge wave

PACS: 84.40.Fe, 13.40.Ks **DOI:** 10.1088/1674-1056/20/2/028401

1. Introduction

Helix traveling wave tubes (TWTs) are broadband and high-gain microwave amplifiers, and are widely used in communications, electronic warfare and radar systems.[1−3] The key method to optimize their structure and improve capability is by studying their nonlinear beam-wave interaction (BWI) characteristics. The current nonlinear theories of TWTs for BWI can be mainly grouped into frequency-domain and time-dependent models.[4,5] CHRISTINE[6−8] stands for the frequency-domain models while GATOR[9−11] represents the time-dependent models.

In this paper, a time-dependent theory of helix TWTs for BWI based on azimuthal symmetry and a sheath helix model is presented. Radio frequency (RF) fields of a slow wave structure (SWS) are treated in terms of a spectral decomposition of the normal modes of the vacuum sheath helix and an overall variation of the form $\exp(k_z z - \omega t)$ is assumed for each wave, where ω and k_z denote the angular frequency and wave number of the vacuum sheath helix, respectively.[9,10] The amplitudes and phases of the RF and space charge (SC) fields are treated to vary in both axial position z and time t. The SC fields are divided into two parts. One is the alternating current (AC) SC field and is treated by solving Poisson's equation combined with the beam continuity equation; the other is the direct current (DC) SC field and is treated by the radial directed self-electric and azimuthally directed self-magnetic fields. Both the solenoidal focusing field and the periodic permanent magnetic (PPM) stack focusing field are included. Frankly speaking, the theory of this paper is just a 2.5-dimensional (2.5-D) model because the RF and SC fields are treated to vary only in radial and axial directions, however, the dynamical equations of electrons are treated in all three directions.

One advantage of this theory over the the theory in Ref. [10] is that the driving sources of RF fields are treated by coupling impedance, which makes this theory more flexible to realize. The hardship of solving physical parameters is avoided by the use of simulation software, such as HFSS[12] and HFCS[13] (which is a module of MTSS[14]). The numerical simulation results of a tube has certified the feasibility of this theory.

*Project supported by the National Natural Science Foundation of China (Grant Nos. 60601004, 60801029, 10876005, and 60931001).

†Corresponding author. E-mail: libin@uestc.edu.cn

© 2011 Chinese Physical Society and IOP Publishing Ltd

2. The general formulations

The general formulations deal with the propagation of an RF signal through a sheath helix in the presence of an electron beam. Both RF fields and SC fields are treated by their corresponding equations. The external focusing fields by means of either a uniform solenoidal magnetic field or a PPM field are also treated.

2.1. The expressions of RF fields

Using Floquet's theorem, the RF field in the SWS, made up of electronic field $\delta\boldsymbol{E}(\boldsymbol{x},t)$ and magnetic field $\delta\boldsymbol{H}(\boldsymbol{x},t)$ can be expressed as

$$\begin{aligned}\delta\boldsymbol{E}(\boldsymbol{x},t) &= \delta\hat{E}(z,t)\mathrm{e}^{\mathrm{i}(k_z z-\omega t+\delta\varphi)}\\ &\quad\times[-\mathrm{i}\,R(r)\,\widehat{r}\,-\beta\Theta(r)\,\widehat{\theta}\,+Z^{(\mathrm{e})}(r)\,\widehat{z}\,],\\ \delta\boldsymbol{H}(\boldsymbol{x},t) &= \delta\hat{E}(z,t)\mathrm{e}^{\mathrm{i}(k_z z-\omega t+\delta\varphi)}\\ &\quad\times[\Theta(r)\,\widehat{r}\,-\mathrm{i}\,\beta R(r)\,\widehat{\theta}\,+\mathrm{i}\,Z^{(\mathrm{b})}(r)\,\widehat{z}\,],\end{aligned}\tag{1}$$

where $R(r)$, $\Theta(r)$, $Z^{(\mathrm{e})}(r)$ and $Z^{(\mathrm{b})}(r)$ are normalized functions of RF fields, and their specific forms are in accord with longitudinal field method (LFM). The factor $\beta=\omega/(ck_z)$ is the normalized phase speed, where c is the speed of light in vacuum. As is is azimuthally symmetric, $\delta\hat{E}$ is related to axial position z and time t but unconcerned with radial position r or angle θ. The $\phi=k_z z-\omega t$ is the phase of field in vacuum while $\delta\phi$ is the phase shift as k_z varies in the presence of electron beam.

Taking the real part of Eq. (1), we can rewrite the RF fields as

$$\begin{aligned}\delta\boldsymbol{E}(\boldsymbol{x},t)&=\delta\hat{E}^{(1)}\boldsymbol{e}(\boldsymbol{x},t)+\delta\hat{E}^{(2)}\boldsymbol{e}^{*}(\boldsymbol{x},t),\\ \delta\boldsymbol{H}(\boldsymbol{x},t)&=\delta\hat{E}^{(1)}\boldsymbol{b}(\boldsymbol{x},t)+\delta\hat{E}^{(2)}\boldsymbol{b}^{*}(\boldsymbol{x},t),\end{aligned}\tag{2}$$

where the eigenvectors are

$$\begin{aligned}\boldsymbol{e}(\boldsymbol{x},t)&=\{R(r)\,\widehat{r}\,\sin\varphi-[\beta\Theta(r)\,\widehat{\theta}\,-Z^{(\mathrm{e})}(r)\,\widehat{z}\,]\cos\varphi\},\\ \boldsymbol{b}(\boldsymbol{x},t)&=\{\Theta(r)\,\widehat{r}\,\cos\varphi+[\varepsilon(r)\beta R(r)\,\widehat{\theta}\,-Z^{(\mathrm{b})}(r)\,\widehat{z}\,]\sin\varphi\},\\ \boldsymbol{e}^{*}(\boldsymbol{x},t)&=\{R(r)\,\widehat{r}\,\cos\varphi+[\beta\Theta(r)\,\widehat{\theta}\,-Z^{(\mathrm{e})}(r)\,\widehat{z}\,]\sin\varphi\},\\ \boldsymbol{b}^{*}(\boldsymbol{x},t)&=\{-\Theta(r)\,\widehat{r}\,\sin\varphi+[\varepsilon(r)\beta R(r)\,\widehat{\theta}\,-Z^{(\mathrm{b})}(r)\,\widehat{z}\,]\cos\varphi\},\end{aligned}\tag{3}$$

and the relationships between them are

$$\begin{aligned}&\boldsymbol{\nabla}\times\boldsymbol{e}+\frac{1}{c}\frac{\partial\boldsymbol{b}}{\partial t}=\boldsymbol{\nabla}\times\boldsymbol{e}^{*}+\frac{1}{c}\frac{\partial\boldsymbol{b}^{*}}{\partial t}=0,\\ &\boldsymbol{\nabla}\times\boldsymbol{b}-\varepsilon(r)\frac{1}{c}\frac{\partial\boldsymbol{e}}{\partial t}=\boldsymbol{\nabla}\times\boldsymbol{b}^{*}-\varepsilon(r)\frac{1}{c}\frac{\partial\boldsymbol{e}^{*}}{\partial t}=0,\end{aligned}\tag{4}$$

while the relationships between amplitudes are

$$\begin{aligned}\delta\hat{E}^{(1)}&=\delta\hat{E}\cos\varphi,\\ \delta\hat{E}^{(2)}&=\delta\hat{E}\sin\varphi,\\ \delta\hat{E}^{2}&=\delta\hat{E}^{(1)2}+\delta\hat{E}^{(2)2}.\end{aligned}\tag{5}$$

The axial components of the fields are in the form of a modified Bessel function[7]

$$\begin{aligned}Z^{(\mathrm{e})}(r)&=\mathrm{I}_0(\gamma r),\\ Z^{(\mathrm{b})}(r)&=\frac{c\gamma\mathrm{I}_0(\gamma r_{\mathrm{h}})\mathrm{I}_0(\gamma r)}{\omega\mathrm{I}_1(\gamma r_{\mathrm{h}})},\end{aligned}\tag{6}$$

where $\gamma=\sqrt{k_z^2-\omega^2/c^2}$ is the propagation factor and r_{h} is the helix radius. Obtaining the axial fields, we can calculate the transverse fields by LFM as

$$\begin{aligned}\gamma^2 e_r&=-\mathrm{i}\,k_z\frac{\partial}{\partial r}e_z,\\ \gamma^2 e_\theta&=\mathrm{i}\,\frac{\omega}{c}\frac{\partial}{\partial r}b_z,\\ \gamma^2 b_r&=-\mathrm{i}\,k_z\frac{\partial}{\partial r}b_z,\\ \gamma^2 b_\theta&=-\mathrm{i}\,\frac{\omega}{c}\frac{\partial}{\partial r}e_z,\end{aligned}\tag{7}$$

2.2. The physical parameters in BWI

The TWTs amplify RF signals so the energy transported is determined by the Poynting flux (i.e. power), the stored energy and the group speed.[10] Therefore, the equations of the RF fields are embodied by the variation of these three physical parameters. As the coupling impedance determines the energy exchange capability of the SWS, it is also needed in the BWI theory.

The power p for each signal denotes the time-averaged Poynting flux over the entire cross-section of the SWS and can be expressed as

$$p=\frac{c}{4\pi}\frac{1}{T}\int_T \mathrm{d}t\iint_A \delta\boldsymbol{E}\times\delta\boldsymbol{B}\cdot\mathrm{d}s,\tag{8}$$

where T is the time period of the signal. Using Eq. (1),

we can rewrite the power as

$$p = S\delta\hat{E}^2. \tag{9}$$

In the similar way, the energy transport W for each signal denotes the time-averaged energy density per unit axial length over the entire cross-section of the SWS and can be expressed as

$$W = \frac{1}{T}\int_T \mathrm{d}t \frac{1}{8\pi}\iiint_V (\delta\boldsymbol{H}\cdot\delta\boldsymbol{B} + \delta\boldsymbol{E}\cdot\delta\boldsymbol{D})\mathrm{d}V, \tag{10}$$

and the energy transported is rewritten as

$$W = U\delta\hat{E}^2. \tag{11}$$

The group speed v_g of a signal denotes its energy transport speed, and can be expressed as

$$v_\mathrm{g} = p/W = S/U. \tag{12}$$

The expression $Z_\mathrm{c}(r)$ denotes the coupling impedance in radial position r and can be given by using Eq. (1) as

$$Z_\mathrm{c}(r) = \frac{|\delta\hat{E}Z^{(\mathrm{e})}(r)|^2}{2k_z^2 p} = \frac{|\mathrm{I}_0(\gamma r)|^2}{2k_z^2 S}, \tag{13}$$

where $\mathrm{I}_0(\gamma r)$ is the zero-order modified Bessel function.

2.3. The equations of RF fields

The RF fields in the presence of beam current are treated as the superposition of the modes in a vacuum. Assuming that they vary slowly in z and t, the equations of the signal's magnitudes are obtained in a manner analogous to the derivation of Poynting's theorem.[9−11]

The RF fields' expression can be rewritten when the magnitudes are normalized by S as

$$\begin{aligned}\delta\boldsymbol{E}(\boldsymbol{x},t) &= \hat{a}^{(1)}\boldsymbol{e}(\boldsymbol{x},t)/S^{1/2} + \hat{a}^{(2)}\boldsymbol{e}^*(\boldsymbol{x},t)/S^{1/2},\\ \delta\boldsymbol{H}(\boldsymbol{x},t) &= \hat{a}^{(1)}\boldsymbol{b}(\boldsymbol{x},t)/S^{1/2} + \hat{a}^{(2)}\boldsymbol{b}^*(\boldsymbol{x},t)/S^{1/2},\end{aligned} \tag{14}$$

where the normalized magnitudes are

$$\begin{aligned}\hat{a} &= S^{1/2},\\ \hat{a}^{(1)} &= \hat{a}\cos\delta\varphi,\\ \hat{a}^{(2)} &= \hat{a}\sin\delta\varphi.\end{aligned} \tag{15}$$

It is assumed that the eigenvectors satisfy Maxwell equations either in the absence or in the presence of a beam. Then Ampère's law and Faraday's law can be expressed as

$$\begin{aligned}&\boldsymbol{\nabla}\times[\hat{a}^{(1)}\boldsymbol{b}/S^{1/2} + \hat{a}^{(2)}\boldsymbol{b}^*/S^{1/2}] - \frac{\varepsilon(r)}{c}\frac{\partial}{\partial t}[\hat{a}^{(1)}\boldsymbol{e}/S^{1/2} + \hat{a}^{(2)}\boldsymbol{e}^*/S^{1/2}] = \frac{4\pi}{c}\boldsymbol{j},\\ &\boldsymbol{\nabla}\times[\hat{a}^{(1)}\boldsymbol{e}/S^{1/2} + \hat{a}^{(2)}\boldsymbol{e}^*/S^{1/2}] + \frac{1}{c}\frac{\partial}{\partial t}[\hat{a}^{(1)}\boldsymbol{b}/S^{1/2} + \hat{a}^{(2)}\boldsymbol{b}^*/S^{1/2}] = 0,\end{aligned} \tag{16}$$

where $\boldsymbol{j}$ denotes the density of the source current. Taking the inner product of $\boldsymbol{b}$ and $\boldsymbol{b}^*$ with Faraday's law and $\boldsymbol{e}$ and $\boldsymbol{e}^*$ with Ampère's law, then integrating the results over the cross section of SWS and averaging over the axial length λ (i.e. the wave length), we can express the equations of the RF fields as

$$\begin{aligned}\left(\frac{\partial}{\partial t} + v_\mathrm{g}\frac{\partial}{\partial z}\right)\hat{a}^{(1)} &= -\frac{k_z v_\mathrm{g}}{4\pi}\int_{z-\pi/k_z}^{z+\pi/k_z}\mathrm{d}z'\iint_A S^{-1/2}\boldsymbol{j}\cdot\boldsymbol{e}\mathrm{d}s,\\ \left(\frac{\partial}{\partial t} + v_\mathrm{g}\frac{\partial}{\partial z}\right)\hat{a}^{(2)} &= -\frac{k_z v_\mathrm{g}}{4\pi}\int_{z-\pi/k_z}^{z+\pi/k_z}\mathrm{d}z'\iint_A S^{-1/2}\boldsymbol{j}\cdot\boldsymbol{e}^*\mathrm{d}s.\end{aligned} \tag{17}$$

Substituting Eq. (13) into Eq. (17), we obtain the following equations for the RF fields:

$$\begin{aligned}\left(\frac{\partial}{\partial t} + v_\mathrm{g}\frac{\partial}{\partial z}\right)\hat{a}^{(1)} &= -\frac{k_z v_\mathrm{g}\sqrt{2Z_\mathrm{c}(z,0)}}{4\pi}\int_{z-\pi/k_z}^{z+\pi/k_z}\mathrm{d}z'\iint_A \mathrm{I}_0(\gamma r)\boldsymbol{j}\cdot\boldsymbol{e}\mathrm{d}s,\\ \left(\frac{\partial}{\partial t} + v_\mathrm{g}\frac{\partial}{\partial z}\right)\hat{a}^{(2)} &= -\frac{k_z v_\mathrm{g}\sqrt{2Z_\mathrm{c}(z,0)}}{4\pi}\int_{z-\pi/k_z}^{z+\pi/k_z}\mathrm{d}z'\iint_A \mathrm{I}_0(\gamma r)\boldsymbol{J}\cdot\boldsymbol{e}^*\mathrm{d}s,\end{aligned} \tag{18}$$

where $Z_\mathrm{c}(z,0)$ is the coupling impedance on axis (i.e $r = 0$).

There is one advantage over Ref. [10] in the RF field equations. The parameters $v_{\rm g}$, k_z and $Z_{\rm c}(z,0)$ can be calculated using HFSS or HFCS, which avoids calculating S and U. By means of $Z_{\rm c}(z,0)$, this time-dependent theory is more flexible and may be used on all kinds of helix TWTs.

2.4. The DC space charge fields

The DC SC fields are self-electronic $\boldsymbol{E}^{(\rm dc)}$ and self-magnetic $\boldsymbol{B}^{(\rm dc)}$ and can be calculated by the equations $\boldsymbol{\nabla}\cdot\boldsymbol{E}^{(\rm dc)}=4\pi\rho$ and $\boldsymbol{\nabla}\times\boldsymbol{B}^{(\rm dc)}=4\pi\boldsymbol{j}/c$ respectively, where ρ is the charge distribution of the electron beam. In the unusual case where a flat-top beam is used, the $\boldsymbol{E}^{(\rm dc)}$ and $\boldsymbol{B}^{(\rm dc)}$ are given by

$$\begin{aligned}\boldsymbol{E}^{(\rm dc)} &= -\,\widehat{r}\,\frac{\omega_{\rm b}^2}{2|\eta_0|}\begin{cases} r, & 0\le r<r_{\rm b},\\ \dfrac{r_{\rm b}^2}{r}, & r\ge r_{\rm b},\end{cases}\\ \boldsymbol{B}^{(\rm dc)} &= -\,\widehat{\theta}\,\frac{\omega_{\rm b}^2}{2|\eta_0|}\frac{v_{z0}}{c}\begin{cases} r, & 0\le r<r_{\rm b},\\ \dfrac{r_{\rm b}^2}{r}, & r\ge r_{\rm b},\end{cases}\end{aligned}\tag{19}$$

where $\omega_{\rm b}$, $r_{\rm b}$ and v_{z0} are the plasma frequency, radius and initial axial velocity of the beam, respectively, and η_0 is the charge-to-mass ratio of a static electron.

The existence of $\boldsymbol{E}^{(\rm dc)}$ means that the beam energy will be depressed, which modifies the initial relativistic factor at a given radius as

$$\gamma_0=\gamma_{\rm ca}-\frac{\omega_{\rm b}^2}{4c^2}\Big(r_{\rm b}^2-r^2+2\ln\frac{r_{\rm h}}{r_{\rm b}}\Big),\tag{20}$$

where $\gamma_{\rm ca}$ is the relativistic factor related to the cathode-to-helix voltage.

2.5. The AC space charge fields

The AC space charge fields are treated by SC waves[2,10] whose amplitudes and phases are assumed to vary slowly in z and t. In the sheath helix model, the SC fields governed by LFM can also be treated as being azimuthally symmetrized and given as

$$\begin{aligned}\boldsymbol{E}^{(\rm sc)}(r,z,t) &= \Big(-\,{\rm i}\,\frac{1}{k_z}\frac{\partial}{\partial r}\hat{E}_z^{(\rm sc)}\hat{e}_r+\hat{E}_z^{(\rm sc)}\hat{e}_z\Big)\\ &\quad\times{\rm e}^{{\rm i}(k_z z-\omega t+\delta\phi^{(\rm sc)})},\end{aligned}\tag{21}$$

where $\boldsymbol{E}^{(\rm sc)}(r,z,t)$ satisfies the Holmholtz equations as

$$\Big(\nabla^2-\frac{1}{c^2}\frac{\partial^2}{\partial^2 t}\Big)\boldsymbol{E}^{(\rm sc)}=4\pi\Big(\frac{1}{c^2}\frac{\partial}{\partial t}+\nabla\rho\Big),\tag{22}$$

where $\delta\phi^{(\rm sc)}$ is the phase shift of space-charge wave.

Combining Poisson's equation with the current continuity equation, the relation between the SC fields and beam current density can be given by

$$\frac{\partial}{\partial t}\boldsymbol{E}^{(\rm sc)}=-4\pi\boldsymbol{j}.\tag{23}$$

An overall variation of the form $\exp(k_z z-\omega t)$ is assumed for the ρ and $\boldsymbol{j}$, so the axial part of the SC fields satisfies the equation

$$\begin{aligned}&\nabla_\perp^2\hat{E}_z^{(\rm sc)}+\Big(\frac{\omega^2}{c^2}-k_z^2\Big)\hat{E}_z^{(\rm sc)}\\ &=-\,{\rm i}\,\frac{4\pi}{\omega}\Big(\frac{\omega^2}{c^2}-k_z^2\Big)j_z.\end{aligned}\tag{24}$$

The sheath helix boundary condition for the SC fields is given by

$$\boldsymbol{E}_z^{(\rm sc)}=0\quad(r=r_{\rm h}).\tag{25}$$

Solving Eq. (24) using Eq. (25), we obtain the following AC SC fields

$$\begin{aligned}\boldsymbol{E}^{(\rm sc)}(r,z,t) &= \hat{E}^{(\rm sc)}\sum_{m=1}^{\infty}({\rm i}\,\tau_m{\rm J}_1(\tau_m r)\,\widehat{r}\\ &\quad+k_z{\rm J}_0(\tau_m r)){\rm e}^{{\rm i}(k_z z-\omega t+\delta\varphi^{(\rm sc)})},\end{aligned}\tag{26}$$

where ${\rm J}_0(\tau_m r)$ and ${\rm J}_1(\tau_m r)$ are Bessel functions of order zero and order one, respectively, and $\tau_m=\chi_{0m}/r_{\rm h}$, χ_{0m} is the m-th root of ${\rm J}_0$ (i.e. ${\rm J}_0(\chi_{0m})=0$).

Taking the real part of Eq. (26), we can write the AC SC fields as

$$\begin{aligned}\boldsymbol{E}^{(\rm sc)}(r,z,t) &= \hat{E}_1^{(\rm sc)}(z,t)\boldsymbol{e}_1^{(\rm sc)}(r,z,t)\\ &\quad+\hat{E}_2^{(\rm sc)}(z,t)\boldsymbol{e}_2^{(\rm sc)}(r,z,t),\end{aligned}\tag{27}$$

where

$$\begin{aligned}\boldsymbol{e}_1^{(\rm sc)}(r,z,t)&=-R^{(\rm sc)}(r)\,\widehat{r}\sin\varphi+Z^{(\rm sc)}(r)\,\widehat{z}\cos\varphi,\\ \boldsymbol{e}_2^{(\rm sc)}(r,z,t)&=-R^{(\rm sc)}(r)\,\widehat{r}\cos\varphi-Z^{(\rm sc)}(r)\,\widehat{z}\sin\varphi,\end{aligned}\tag{28}$$

and represent

$$\begin{aligned}R^{(\rm sc)}(r)&=\sum_{m=1}^{\infty}\tau_m{\rm J}_1(\tau_m r),\\ Z^{(\rm sc)}(r)&=\sum_{m=1}^{\infty}k_z{\rm J}_0(\tau_m r).\end{aligned}\tag{29}$$

Under the assumption of $\partial\hat{E}^{(\rm sc)}/\partial t\ll\omega\hat{E}^{(\rm sc)}$ and substituting Eq. (27) into Eq. (28), we can obtain the equations of AC SC fields as

$$\hat{E}_1^{(\rm sc)}\dot{\boldsymbol{e}}_1^{(\rm sc)}+\hat{E}_2^{(\rm sc)}\dot{\boldsymbol{e}}_2^{(\rm sc)}=-\frac{4\pi\boldsymbol{j}}{\omega},\tag{30}$$

where

$$\begin{pmatrix} \dot{\boldsymbol{e}}_1^{(\mathrm{sc})}(r,z,t) \\ \dot{\boldsymbol{e}}_2^{(\mathrm{sc})}(r,z,t) \end{pmatrix} = \widehat{z}\, R^{(\mathrm{sc})}(r) \begin{pmatrix} \cos\phi \\ -\sin\phi \end{pmatrix} + \widehat{z}\, Z^{(\mathrm{sc})}(r) \begin{pmatrix} \sin\phi \\ \cos\phi \end{pmatrix}. \quad (31)$$

In a similar way as the RF equations were obtained, the expression (30) is treated by the following steps: taking the inner product of $\dot{\boldsymbol{e}}_1^{(\mathrm{sc})}$ and $\dot{\boldsymbol{e}}_2^{(\mathrm{sc})}$; integrating the result over the entire cross section of the SWS; averaging the result over the axial length of the wavelength. Then the equations of the AC SC fields can be given by

$$\hat{E}_i^{(\mathrm{sc})} = -\frac{8k_z}{\omega r_{\mathrm{h}}^2} \sum_{m=1}^{\infty} \int_{z-\pi/k_z}^{z+\pi/k_z} \mathrm{d}z' \oint \mathrm{d}S \times \frac{\boldsymbol{j}(\boldsymbol{x}_\perp, z', t) \cdot \boldsymbol{e}_i^{(\mathrm{sc})}(\boldsymbol{x}_\perp, z', t)}{(\tau_m^2 + k_z^2)\mathrm{J}_1^2(\tau_m r_{\mathrm{h}})}, \quad (i = 1, 2). \quad (32)$$

It should be noted that in the AC SC fields equations (32), m is the number of radial modes whose appropriate value may vary widely. Hence, in practice, the value of m is added until convergence is reached.

2.6. The external focusing fields

There are two types of focusing fields in TWTs. One is the solenoidal field produced by coils and given by

$$\boldsymbol{B}_{\mathrm{ext}} = B_0\, \widehat{z}, \quad (33)$$

where B_0 is the amplitude of the focusing field.

The other is the PPM field presented as

$$\boldsymbol{B}_{\mathrm{ext}} = B_{\mathrm{w}} \left[\widehat{r}\, \frac{k_{\mathrm{w}} r}{2} \sin(k_{\mathrm{w}} z) + \widehat{z} \cos(k_{\mathrm{w}} z) \right], \quad (34)$$

where B_{w} is the on-axial (i.e. $r = 0$) magnetic amplitude and $k_{\mathrm{w}} = 2\pi/\lambda_{\mathrm{w}}$ (where λ_{w} is the PPM period) is the PPM "wave number".

2.7. The equations of motion

The electrons' equations of motion are obtained by combining the field equations (i.e. the RF field equations, the SC field equations and the focusing field equations) with relativistic Lorentz equations. As the self-magnetic fields can be ignored when comparing them with the magnetic RF fields and the focusing fields, the equations of motion are given by

$$\frac{\mathrm{d}}{\mathrm{d}t}\boldsymbol{P} = -e[\delta\boldsymbol{E}(\boldsymbol{x}, t) + \boldsymbol{E}^{(\mathrm{sc})}(\boldsymbol{x}, t)] - \frac{e}{c}\boldsymbol{v} \times [\delta\boldsymbol{B}(\boldsymbol{x}, t) + \boldsymbol{B}_{\mathrm{ext}}], \quad (35)$$

where $\boldsymbol{P}$ and e are the momentum and charge of a particle, respectively. For convenience, the SC fields are assumed to be just the AC SC fields while the effect of DC SC fields on electrons is included in the initial beam relativistically expressed in Eq. (20).

3. The numerical results

The sequence for simulating this time-dependent BWI theory is: firstly, set the initial conditions for the electron beam and simulating grids; secondly, calculate the stimulating sources for the RF field and SC field equations by accumulating the electron charge to the grid and averaging over wave length; thirdly, the SC fields are directly calculated, while the RF fields are calculated by the MacCormack method; fourthly, the orbits of the electrons are calculated by solving the equations of motion by the fourth Runge–Kutta method. This procedure is repeated over the time scale.

The SWS chosen for simulation is referred to a helix TWT built at the Northrop–Grumman Corporation. The average radius and pitch of the helix are 1.245 mm and 0.8014 mm, respectively. The wall radius is 2.794 mm and no vanes are loaded in this structure. There are three rods with rectangular cross sections running along the helix. The dielectric constant of the rods is 6.5 and their dimensions are 0.508 mm $\times$1.473 mm. There are some simulated results below.

3.1. Beam propagation

The beam propagation describes the particle trajectories for input power $p_{\mathrm{in}} = 0$ into either a solenoid or PPM Brillouin magnetically focused helix TWT. The specific beam is modeled as an accelerating voltage of $V_{\mathrm{b}} = 2.84$ kV, a current of $I_{\mathrm{b}} = 170$ mA, and an initial radius of $r_{\mathrm{b0}} = 0.5$ mm. The Brillouin field's amplitude of this beam for a solenoid is $B_0 = 952.7$ G (1 G=10^{-4} T) while for a PPM field is $B_{\mathrm{w}} = 1347.3$ G with a period of $p_{\mathrm{w}} = 6.604$ mm.

The beam propagation is shown in Figs. 1 and 2, in which the thick lines denote the average radius of

the helix (i.e. 1.245 mm). The visible flat trajectories of the particles are shown in Fig. 1 while their disciplinary fluctuating form is shown in Fig. 2. It is proved that the beam will form a balanced shape as it travels through a Brillouin focused field.

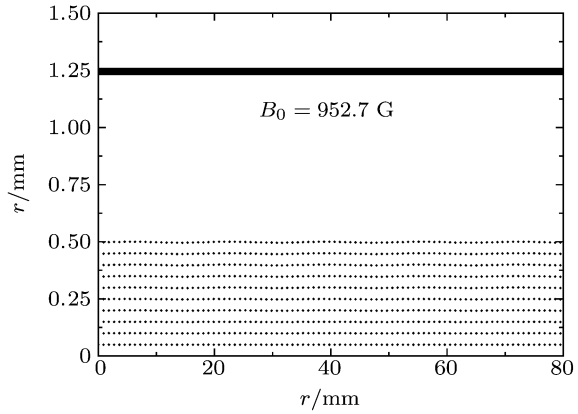


Fig. 1. Propagation of a beam through a solenoidal Brillouin field of $B_0 = 952.7$ G, where $V_\mathrm{b} = 2.84$ kV, $I_\mathrm{b} = 170$ mA and $r_\mathrm{b0} = 0.5$ mm.

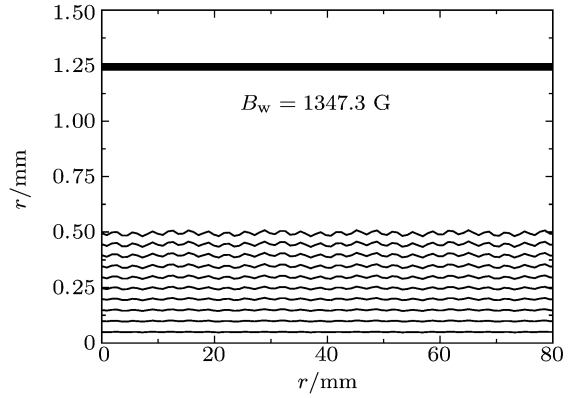


Fig. 2. Propagation of a beam through a PPM Brillouin field of $B_\mathrm{w} = 1347.3$ G with $p_\mathrm{w} = 6.604$ mm, where $V_\mathrm{b} = 2.84$ kV, $I_\mathrm{b} = 170$ mA and $r_\mathrm{b0} = 0.5$ mm.

3.2. The BWI simulations

In the simulation of BWI, a signal with a frequency of $f = 5$ GHz is injected into the beam with a PPM Brillouin field described in Fig. 2.

The evolution of the stable output power p_out with an axial distance z in the case of different p_in is shown in Fig. 3. The results show a saturated power of 130 W, which is very close to GATOR's 131-W saturated power.[10] Especially in the case of $p_\mathrm{in} = 30$ mW, where the saturated distance is 69 mm, which is equal to the value given in the literature.

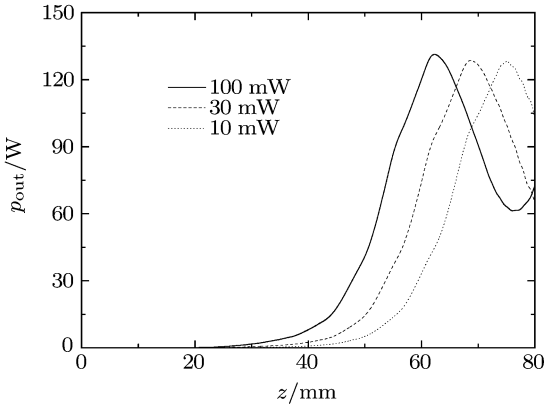


Fig. 3. The evolution of the stable output power p_out with axial distance z by different input power $p_\mathrm{in} = 10, 30, 100$ mW, where $V_\mathrm{b} = 2.84$ kV, $I_\mathrm{b} = 170$ mA and $r_\mathrm{b0} = 0.5$ mm.

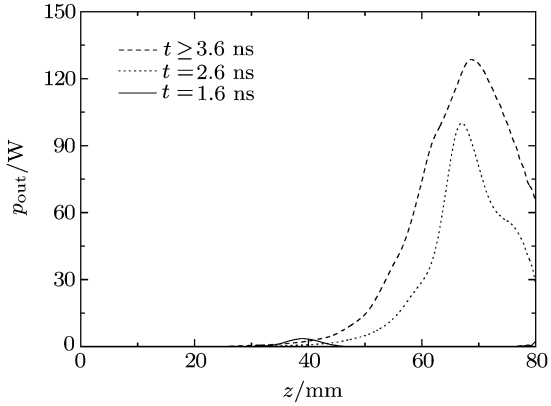


Fig. 4. The evolution of the output power p_out with axial distance z by different time $t = 1.6, 2.6$ ns and $t \geq 3.6$ ns, where p_in is 30 mW, $V_\mathrm{b} = 2.84$ kV, $I_\mathrm{b} = 170$ mA and $r_\mathrm{b0} = 0.5$ mm.

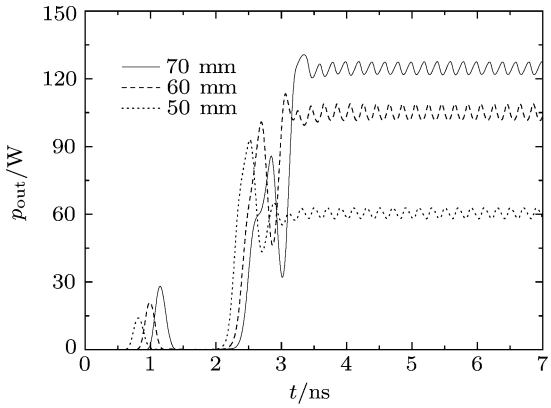


Fig. 5. The evolution of the output power p_out with time t by different axial positions $z = 50$, 60, 70 mm, where p_in is 30 mW, $V_\mathrm{b} = 2.84$ kV, $I_\mathrm{b} = 170$ mA and $r_\mathrm{b0} = 0.5$ mm.

The evolution of the output power p_out with axial distance z in the case of different time t is shown in

Fig. 4. As the input signal propagates at its group speed v_g, the energy exchange between it and the beam is processed along the whole distance until a stability is achieved.

The evolution of output power p_{out} in a fixed axial position z with different time is shown in Fig. 5. The fluctuations in the output power can be stated by two possible reasons. One can be easily explained as the essence of all time-domain theories, which cannot naturally avoid fluctuating outputs. However, by roughly calculating the output curves in Fig. 5, is is found that the fluctuating period is about 0.2 ns, which is so close to the 5-GHz input signal's time period that a second possible reason for the fluctuation may be concluded to be bound up with the frequency of input signal. Finding the exact cause of the fluctuation is interesting and needs to be studied.

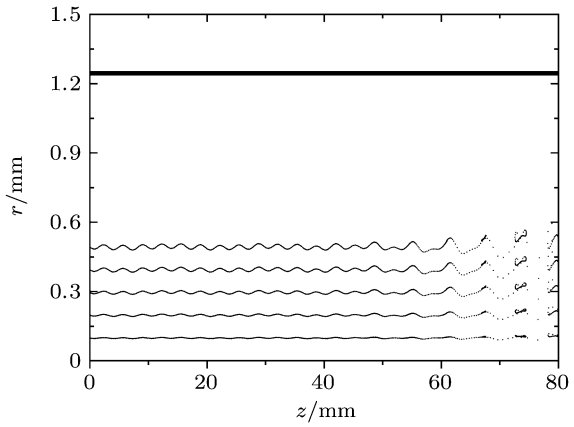


Fig. 6. The stable distribution of the particles' radial position r with axial position z, where p_{in} is 30 mW, $V_b = 2.84$ kV, $I_b = 170$ mA and $r_{b0} = 0.5$ mm.

The distribution of particles in the phase space of radial position r and axial position z are shown in Figs. 6 and 7 when the output power p_{out} is stable, and also with which the interacting phenomenon between wave and beam is described.

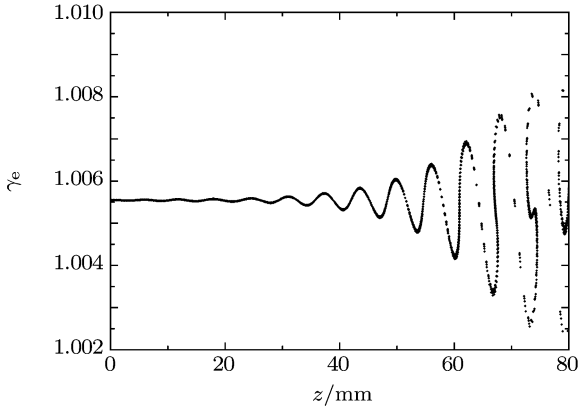


Fig. 7. The stable distribution of the particles' axial speed (described by the electron's axial relativistic γ_e in the figure) with axial position z, where p_{in} is 30 mW, $V_b = 2.84$ kV, $I_b = 170$ mA and $r_{b0} = 0.5$ mm.

4. Conclusions

A three-dimensional time-dependent nonlinear theory of helix TWTs for BWI has been developed in this paper. A single RF wave propagating through the helix is described. The difficulty of solving the complex physical parameters is avoided by using HFCS, which simplifies the simulation and improves its accuracy. The results of the simulation are compared with those from the literature; this certifies the feasibility of our theory. Further, as its equations are in the time domain, this theory can be improved to simulate backward wave oscillation, which will be studied later.

References

[1] Liao F J 2008 *Technology of Vacuum Electronics* (Beijing: National Defense Industry Press) p. 48 (in Chinese)
[2] Liu S G, Li H F, Wang W X and Mo Y L 1985 *Introduction to Microwave Electronics* (Beijing: National Defense Industry Press) p. 330 (in Chinese)
[3] Pierce J R 1950 *Traveling Wave Tubes* (Princeton NJ: Van Nostrand) p. 109
[4] Duan Z Y, Gong Y B, Wei Y Y and Wang W X 2008 *Chin. Phys.* B **17** 2484
[5] Liu P K, Xiong C D and Liu S G 1997 *Acta Phys. Sin.* **46** 892 (in Chinese)
[6] Xiao L 2006 *Ph. D. Distribution* Beijing: Institute of Electronics, Chinese Academy of Sciences (in Chinese)
[7] Chernin D, Antonsen T M Jr, Levush B and Whaley D R 2001 *IEEE Trans. Electron. Dev.* **48** 3
[8] Chernin D P and Antonsen T M Jr 2003 *IEEE Trans. Electron. Dev.* **50** 2540
[9] Freund H P, Zaidman E G and Antonsen T M Jr 1996 *Phys. Plasmas* **3** 3145
[10] Freund H P and Zaidman E G 1997 *Phys. Plasmas* **4** 2292
[11] Freund H P 1999 *Phys. Plasmas* **6** 3633
[12] Lee J F, D K Sun and Cendes Z J 1991 *IEEE Trans. Magn.* **27** 4032
[13] Xu L, Yang Z H and Li B 2009 *IEEE Trans. Electron. Dev.* **56** 1141
[14] Li B, Yang Z H and Li J Q 2009 *IEEE Trans. Electron. Dev.* **56** 919
[15] Li J Q and Mo Y L 2006 *Acta Phys. Sin.* **55** 4117 (in Chinese)
[16] Gao P, Hu Y L, Li B, Li J Q and Yang Z H 2009 *Acta Phys. Sin.* **58** 6665 (in Chinese)